Acta Crystallographica Section B
Structural Science
ISSN 0108-7681

Structure-directing weak phosphoryl *X*H···O═P (*X* = C, N) hydrogen bonds in cyclic oxazaphospholidines and oxazaphosphinanes

A. van der Lee,[a]* M. Rolland,[a] X. Marat,[b] D. Virieux,[b] J.-N. Volle[b] and J.-L. Pirat[b]

[a]Institut Européen des Membranes, UMR 5635, cc 047 Université de Montpellier II, 34095 Montpellier, France, and [b]Institut Charles Gerhardt Montpellier, Architectures Moléculaires et Matériaux Nanostructurés, UMR 5253, ENSCM, 8 rue de l'École Normale, 34296 Montpellier, France

Correspondence e-mail: avderlee@univ-montp2.fr

Received 31 August 2007
Accepted 21 November 2007

The structures of six cyclic oxazaphospholidines and three cyclic oxazaphosphinanes have been determined and their supramolecular structures have been compared. The molecules differ with respect to the functional groups attached to the central five- or six-membered rings, but have one phosphoryl group in common. The predominant feature in the supramolecular structures is the existence of relatively weak intermolecular phosphoryl *X*H···O═P (*X* = C, N) hydrogen bonds, creating in nearly all cases linear zigzag or double molecular chains. The molecular chains are in general linked to each other *via* very weak CH···π or usual hydrogen-bond interactions. A survey of the Cambridge Structural Database on similar *X*H···O═P interactions shows a very large flexibility of the *X*H···O angle, which is in agreement with the DFT calculation reported elsewhere. The strength of the *X*H···O═P interaction can therefore be considered as relatively weak to moderately strong, and is expected to play at least a role in the formation of secondary substructures.

1. Introduction

Over the last few decades there has been considerable interest in phosphorylated compounds because of their remarkable biological applications, such as enzyme inhibitors, antibiotics, antitumorals, herbicides and fungicides (Grembecka *et al.*, 2003). Relatively new synthetic methods, such as the asymmetric synthesis of organophosphorus compounds (Kolodiazhnyi, 1998), have stimulated their development, also because of their great practical value as ligands in catalysis for asymmetric synthesis. To find new chiral compounds as building blocks for parallel chemistry, we developed the synthesis of a rigid chiral cyclic structure, with two bulky phenyl groups, the α-substituted β-keto-oxazaphospholidine oxides (1) as precursors for heterocycles and phosphopep-

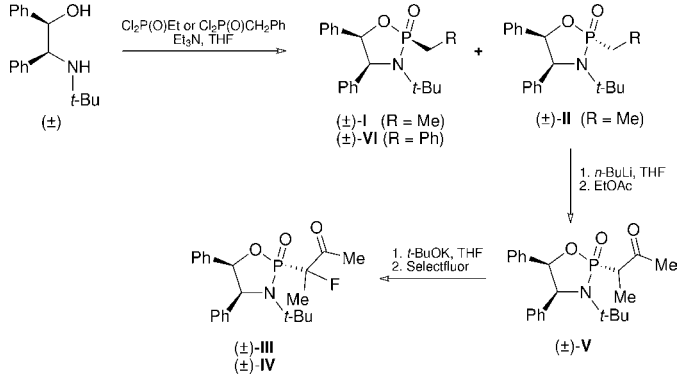

Figure 1
Synthetic route for β-keto-oxazaphospholidine oxides (I)–(VI). Details on the exact stereochemistry can be found in Pirat, Marat *et al.* (2005).

tides. The alkylation or electrophilic fluorination of these compounds proceeds with high stereoselectivity and high yields, and provides an access to pure diastereomers, as illustrated in Fig. 1 (Pirat, Marat *et al.*, 2005).

In parallel, we developed the synthesis of 1,4,2-oxazaphosphinanes (Fig. 2). Such reagents can be considered as an interesting combination of a rigid cyclic structure with two bulky phenyl groups on the same side, and a reactive P—H bond which allows a wide range of reactivity. This intermediate is then very suitable for stereoselective carbon–phosphorus bond formation and gives (VIII) by a two-step sequence with aryl halides in the final reaction (Cristau *et al.*, 2003). The pallado-catalyzed arylation reaction occurs with a complete diastereoselectivity and shows systematic retention of the configuration on the P atom. Subsequently, an epimerization process in acidic conditions of the phosphorus center of (VIII) bearing three phenyl groups, permitted to obtain (VII) with a diastereomeric excess of at least 97%, the latter being an analog in phosphinate series of the antidepressive drug hydroxybupropion.

Apart from the studies that are driven by the molecular context, the supramolecular interactions in these compounds, and notably the weak phosphoryl CH···O hydrogen bonds, are of interest. In the absence of relatively strong classical hydrogen bonds, the O atom of the P═O bond acts as a hydrogen-bond acceptor to form a connected network of hydrogen bonds which holds the structure together. In a CSD (Cambridge Structural Database; Allen, 2002) survey of the distribution of CH···O interactions to phosphoryl P═O groups, a very weak clustering of H···O distances around 2.8 Å was found in the range 2.4–4.0 Å (Forristal *et al.*, 2001). In the latter study one example was shown in which weak phosphoryl CH···O hydrogen-bond interactions resulted in the formation of a beautiful helicoidal structure with a pitch of 52.675 Å. With this in mind we have undertaken a more systematic study of how CH or NH to phosphoryl P═O group interactions can direct the supramolecular structure. The crystal structures of nine oxazaphospholidines and oxazaphosphinanes have been determined by X-ray diffraction (Fig. 3). The series splits naturally in two: the six oxazaphospholidines have a five-membered O═(P—O—C—C—N) ring, molecules (I)–(VI), whereas the three oxazaphosphinanes have a six-membered O═(P—O—C—C—N—C) ring. The attached functional groups vary along the series and offer the possibility of closing or opening the contact possibilities to the donor sites on the ring.

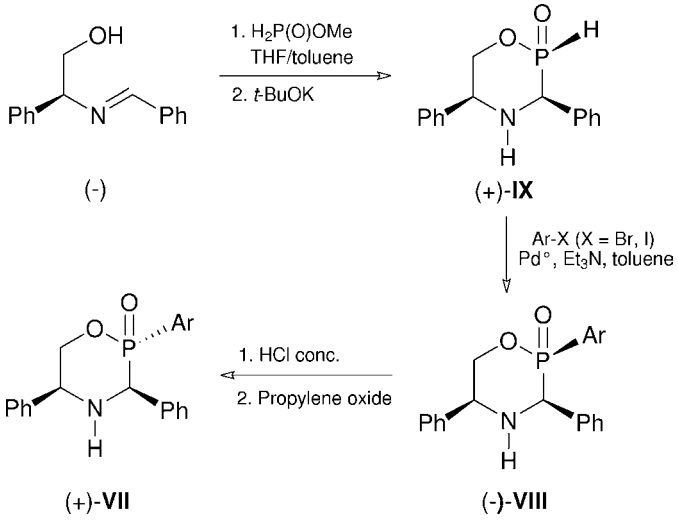

Figure 2
Enantioselective synthetic route for 2-aryl-3,5-diphenyl-[1,4,2]-oxazaphosphinanes (VII), (VIII) and (IX) (Volle *et al.*, 2006).

2. Experimental

2.1. Synthesis

Full details of the syntheses, including ^{1}H, ^{13}C, ^{31}P and ^{19}F NMR data, IR data, HRMS data, and melting points have

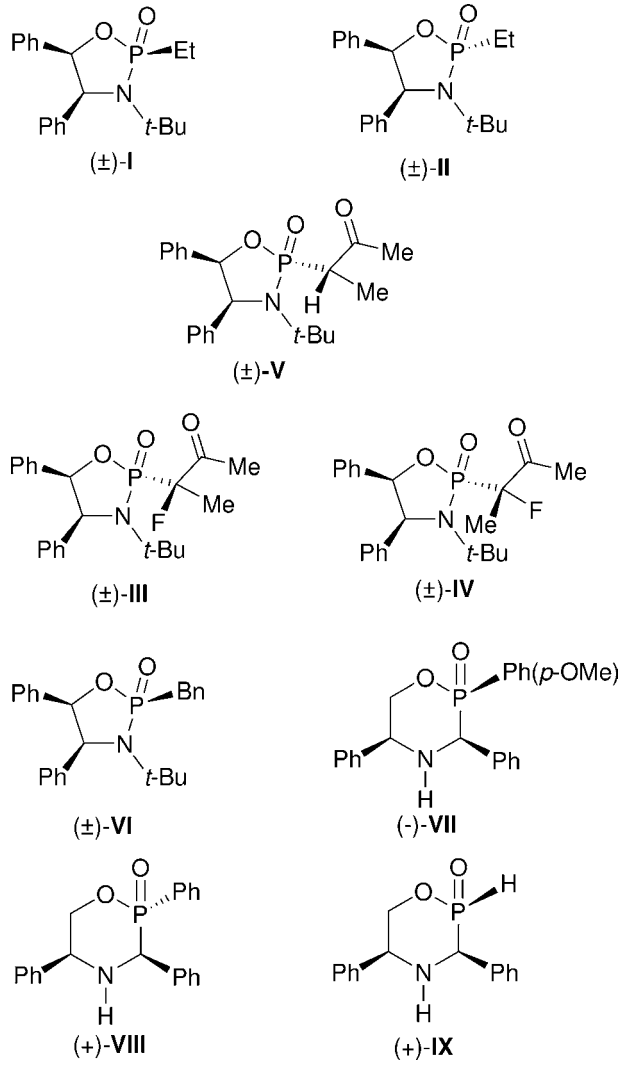

Figure 3
Molecules (I)–(IX), whose three-dimensional structures were determined in this study. Note that the structure of (II) contains two molecules in the asymmetric unit, which were chosen to be each other's enantiomorph.

Table 1
Experimental details.

	(I)	(II)	(VII)	(IX)
Crystal data				
Chemical formula	$C_{20}H_{26}NO_2P$	$C_{20}H_{26}NO_2P$	$C_{22}H_{22}NO_3P$	$C_{15}H_{16}NO_2P$
M_r	343.39	343.39	379.40	273.27
Cell setting, space group	Orthorhombic, *Pbca*	Triclinic, $P\bar{1}$	Monoclinic, $P12_11$	Orthorhombic, $P2_12_12_1$
Temperature (K)	120	120	175	175
a, b, c (Å)	10.5381 (8), 15.7519 (14), 22.626 (2)	6.7231 (5), 11.9766 (6), 23.6865 (16)	10.0104 (3), 8.10560 (10), 12.5372 (3)	5.3914 (2), 11.7559 (4), 21.6032 (8)
α, β, γ (°)	90, 90, 90	97.644 (3), 93.038 (2), 98.742 (2)	90, 109.717 (5), 90	90, 90, 90
V (Å^3)	3755.8 (6)	1863.1 (2)	957.63 (5)	1369.23 (9)
Z	8	4	2	4
D_x (Mg m^{-3})	1.215	1.224	1.316	1.326
Radiation type	Synchrotron, λ = 0.50606 Å	Synchrotron, λ = 0.50606 Å	Mo $K\alpha$	Mo $K\alpha$
μ (mm^{-1})	0.07	0.07	0.17	0.20
Crystal form, colour	Needle, translucent pale white	Needle, translucent pale white	Prism, translucent pale white	Prism, translucent pale white
Crystal size (mm)	0.50 × 0.05 × 0.05	0.40 × 0.05 × 0.05	0.32 × 0.30 × 0.20	0.30 × 0.20 × 0.20
Data collection				
Diffractometer	Bruker SMART	Bruker SMART	Oxford Diffraction XCALIBUR	Oxford Diffraction XCALIBUR
Data collection method	ω	ω	ω	ω
Absorption correction	Multi-scan (based on symmetry-related measurements)	Multi-scan (based on symmetry-related measurements)	Multi-scan (based on symmetry-related measurements)	Multi-scan (based on symmetry-related measurements)
T_{min}	0.89	0.91	0.952	0.940
T_{max}	1.00	1.00	0.967	0.961
No. of measured, independent and observed reflections	22 025, 6228, 4671	32 894, 11 718, 7201	12 688, 5435, 3438	26 882, 4506, 1197
Criterion for observed reflections	$I > 2.0\sigma(I)$	$I > 2.0\sigma(I)$	$I > 2.0\sigma(I)$	$I > 2.0\sigma(I)$
R_{int}	0.072	0.073	0.028	0.057
θ_{max} (°)	20.8	20.9	32.2	32.5
No. and frequency of standard reflections	–	–	25 every 4 frames	25 every 4 frames
Refinement				
Refinement on	F	F	F	F
$R[F^2 > 2\sigma(F^2)]$, $wR(F^2)$, S	0.052, 0.052, 0.99	0.050, 0.053, 1.06	0.048, 0.046, 1.11	0.028, 0.029, 1.11
No. of reflections	4671	7201	3438	1197
No. of parameters	218	434	245	173
H-atom treatment	Constrained to parent site	Constrained to parent site	Constrained to parent site	Constrained to parent site
Weighting scheme	Calculated†	Calculated†	Calculated†	Calculated†
$(\Delta/\sigma)_{max}$	0.001	0.001	< 0.0001	0.014
$\Delta\rho_{max}$, $\Delta\rho_{min}$ (e Å^{-3})	0.36, −0.67	0.48, −0.58	0.23, −0.31	0.12, −0.18
Extinction method	Larson (1970), equation (22)	Larson (1970), equation (22)	None	None
Extinction coefficient	8606.704	660 (90)	–	–
Absolute structure	–	–	Flack (1983), 2104 Friedel pairs	Flack (1983), 1866 Friedel pairs
Flack parameter	–	–	0.18 (12)	−0.10 (16)

Computer programs used: *SMART*, *SAINT* (Siemens, 1993), *CrysAlis* (Oxford Diffraction, 2006), *SIR*92 (Altomare *et al.*, 1994), *SIR*2002 (Burla *et al.*, 2003), *CRYSTALS* (Betteridge *et al.*, 2003), *CAMERON* (Watkin *et al.*, 1996), *BAYMEM* (van Smaalen *et al.*, 2003). † Part 1, Chebychev polynomial (Watkin, 1994; Prince, 1982); [weight] = $1.0/[A_0^* T_0(x) + A_1^* T_1(x) \ldots + A_{n-1}]T_{n-1}(x)]$, where A_i are the Chebychev coefficients listed below and $\times = F/F_{max}$. Method = robust weighting (Prince, 1982); $W = [\text{weight}][1 - (\delta F/6\sigma F)^2]^2$. A_i are: 0.490, 0.521, 0.215 for (I); 0.507, 0.574, 0.220 for (II); 18.4, −27.6, 15.3, −5.81 for (VII); 27.8, −41.7, 34.0, −14.2, 6.83 for (IX).

been reported by Pirat, Monbrun *et al.* (2005) for (I)–(VI) and by Volle *et al.* (2006) for (VII)–(IX).

2.2. Data collection, structure solution and refinement

X-ray data were collected with Mo $K\alpha$ radiation (λ = 0.71073 Å) for (III)–(IX) using a Siemens P3, an Enraf–Nonius CAD4 and an Oxford Diffraction Xcalibur-I diffractometer. Graphite-monochromated radiation was used in all cases. Data for (I)–(II) were collected at beamline ID11 of the European Synchrotron Radiation Facility using a wavelength of 0.50606 Å and a Bruker SMART diffractometer. Most of the crystals crystallized as tiny needles, which makes the data quality in certain cases very mediocre, especially for (III)–(VI) and (VIII). These structures will not be discussed in detail here; detailed data can be obtained *via* the accompanying cif

Table 2
Hydrogen-bond parameters (Å, °).

D—H···A	D—H	H···A	D···A	D—H···A	Acceptor motif
(I)					
C4—H25···O6^{i}	0.96	2.40	3.244 (2)	146	Phosphoryl
(II)					
C4—H50···O6^{ii}	0.94	2.28	3.196(3)	165	Phosphoryl
C28—H75···O30^{iii}	0.93	2.27	3.179 (3)	165	Phosphoryl
(VII)					
N4—H31···O7^{iv}	0.93	2.54	3.089(3)	118	Phosphoryl
C3—H32···O7^{iv}	0.99	2.57	3.153 (4)	118	Phosphoryl
C21—H44···O14^{v}	0.93	2.60	3.286 (4)	131	Methoxy
(IX)					
N4—H22···O7^{vi}	1.05	1.96	2.916 (2)	149	Phosphoryl
C18—H34···*Cg*3^{vii}†	0.93	2.96	3.647 (3)	132	π system

Symmetry codes: (i) $\frac{1}{2}+x, y, \frac{1}{2}-z$; (ii) $-1+x, y, z$; (iii) $1-x, -y, -z$; (iv) $-x, -\frac{1}{2}+y, 1-z$; (v) $1-x, -\frac{1}{2}+y, 2-z$; (vi) $1-x, \frac{1}{2}+y, \frac{3}{2}-z$; (vii) $-x, \frac{1}{2}+y, \frac{3}{2}-z$. † *Cg*3 is the centroid of ring C8–C13 in molecule (IX).

files; molecular drawings are available *via* the supplementary material. However, the resulting packings will be qualitatively discussed in the present context of a study of weak phosphorous CH···O interactions.

The structures were solved by direct methods using *SIR*92 (Altomare *et al.*, 1994) or *SIR*2002 (Burla *et al.*, 2003) for (I)–(II), and (IX), and by the *ab initio* charge-flipping method using *BAYMEM* (van Smaalen *et al.*, 2003) for (VII) using default values for the flipping parameters. In order to determine the absolute configuration the Flack parameter was refined for the two non-centrosymmetric structures, but in view of the experimental standard deviations the refined value, which was not far from zero in all cases, may not be very reliable. A Chebyshev polynomial (Watkin, 1994; Prince, 1982) was used in the weighting scheme $w = [1- ((F_{obs} - F_{calc})/6\sigma(F))^2]^2/[A_0T_0(x) + A_1T_1(x) \ \ldots \ + A_{n-1}T_{n-1}(x)]$, where A_i are the Chebychev coefficients listed in Table 1 and $x = F_{calc}/F_{max}$.

All the structure refinements were carried out with the *CRYSTALS* package (Betteridge *et al.*, 2003): the H atoms were initially refined with soft restraints on the bond lengths and angles to regularize their geometry and U_{iso}(H) in the range 1.2–1.5 × U_{eq} of the parent atom, after which the positions were refined with riding constraints. In some cases, however, and notably for H atoms involved in weak bonding interactions, the geometry was not optimized using soft restraints, but instead their positions found from the difference-Fourier map were used for letting them ride on the parent atoms. The analyses of the supramolecular structures were carried out with the aid of *CRYSTALS*, *PLATON* (Spek, 2003) and *MERCURY* (Macrae *et al.*, 2006), and the structural drawings were produced using *CAMERON* (Watkin *et al.*, 1996). Other details of cell data, data collection and refinement are summarized in Table 1, as well as the details of the software employed (Siemens, 1993, 1995; Oxford Diffraction, 2006). Details of the hydrogen-bond geometry are given in Table 2.

[1] Supplementary data for this paper are available from the IUCr electronic archives (Reference: GP5020). Services for accessing these data are described at the back of the journal.

3. Results and discussion

3.1. Molecular configuration

Fig. 4 shows the atom labelling of the central rings and the chiral centers of the structures (I)–(IX). The chiral centers in

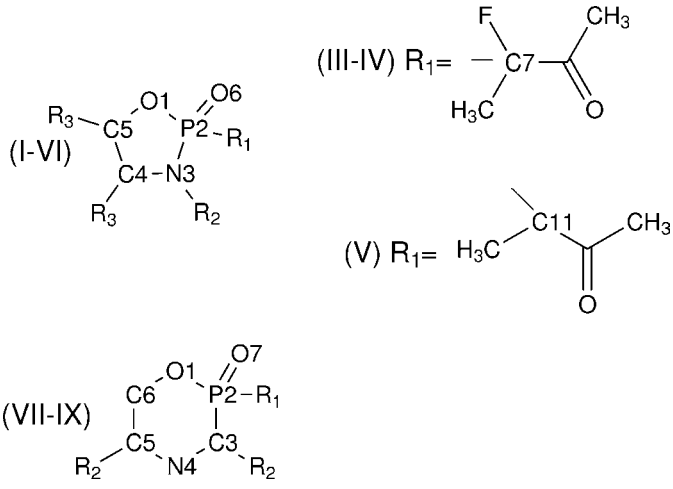

Figure 4
Atom labelling of the central rings and the chiral centers for structures (I)–(IX). Note that the labelling of the second independent molecule in the asymetric unit of (II) follows the same systematic as that depicted in this figure, *i.e.* O1—C5 is replaced by O25—C29.

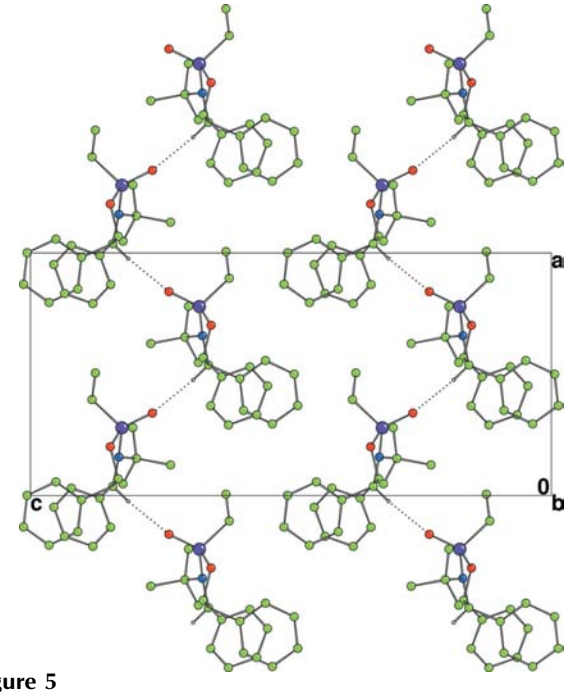

Figure 5
Part of the crystal structure of (I) showing one-dimensional chains running along the *a* axis. The H atoms that do not take part in the bonding interactions have been omitted for the sake of clarity in this and all subsequent drawings.

molecules (I)–(VI) are P2, C4 and C5; in (III) and (IV) additionally C7; in (V) additionally C11; in (II) additionally P26, C28 and C29, because it is a $Z' = 2$ structure. All structures (I)–(VI) are centrosymmetric; (I) and (II) are diastereomers with an *RSR* configuration for molecule (I) drawn in Fig. sup-ii of the supplementary data, and (±)-*RRS* and (±)-*SSR* configurations for the first (P2, C4 and C5) and second molecule (P25, C28 and C29) (II) in the asymmetric unit, respectively (Fig. sup-ii of the supplementary data). Compounds (III) and (IV) are also diastereomers with configurations (±)-*SSRS* and (±)-*RRSS* for the molecules drawn in Fig. sup-iii and Fig. sup-iv, respectively, of the supplementary data. It was not possible to grow crystals of the diastereomers for (V) and (VI) of sufficient quality; the configurations presented here are (±)-*RRSR* and (±)-*RSR*, respectively (Figs. sup-v and sup-vi for (V) and (VI), respectively, of the supplementary data).

The chiral centers in molecules (VII)–(IX) are P2, C3 and C5, respectively. The structures are non-centrosymmetric, thus only one enantiomer is present. Molecule (VII) in Fig. sup-vii of the supplementary data has an *RSS* configuration, molecule (VIII) in Fig. sup-viii an *SSS* configuration and molecule (IX) in Fig. sup-ix an *RSS* configuration. The P═O double-bond distance varies between 1.459 (6) Å for molecule (V) and 1.51 (2) Å for molecule (III), in good agreement with DFT calculations on similar compounds (1.491 Å; Henn *et al.*, 2004).

3.2. Supramolecular structures

3.2.1. (±)-(2*R*,4*S*,5*R*)-3-*tert*-Butyl-2-ethyl-4,5-diphenyl-1,3,2-oxazaphospholidine 2-oxide (I). Molecules of (I) are linked into linear molecular chains running along the *a* axis by weak hydrogen bonds [$D\cdots A$ = 3.244 (2) Å and DH$\cdots A$ = 146°] between the phosphoryl O6-atom acceptor and the H25 atom, which is on the opposite side of the oxazaphospholidine ring. The infinite hydrogen-bonded chain is a $C(5)$ chain according to the classification of Bernstein *et al.* (1995). There are four molecular chains running through each unit cell, of which only two are shown in Fig. 5 for the sake of clarity; the molecular chains in Fig. 5 have their phenyl moieties in a staggered conformation, whereas in a 90° rotated view down the *c* axis the *tert*-butyl groups are staggered. There are no weak bonding interactions between the molecular chains.

3.2.2. (2*S*,4*S*,5*R*)- and (2*R*,4*R*,5*S*)-3-*tert*-Butyl-2-ethyl-4,5-diphenyl-1,3,2-oxazaphospholidine 2-oxide (II). The two independent molecules of (II) are like its diastereomer (I) linked by weak hydrogen bonds into infinite linear $C(5)$ chains running along the *a* axis. The phosphoryl oxygen O6 and O30 atoms act as acceptors and are hydrogen bonded to the H50 and H75 atoms located on the opposite side of neighbouring oxazaphospholidine rings. The hydrogen-bond donor C atoms, C4 and C28, respectively, are exactly the same as in molecule (I). The hydrogen-bonding motif is, however, different. Whereas in the structure of molecule (I), Fig. 5, the hydrogen bonds are in a zigzag configuration, in the structure of (II) they are nearly linear and follow the chain direction. As is clearly seen in Fig. 6, the chains are on one side in a staggered conformation with respect to the phenyl moieties on C4, whereas on the other side they are staggered with the ethyl

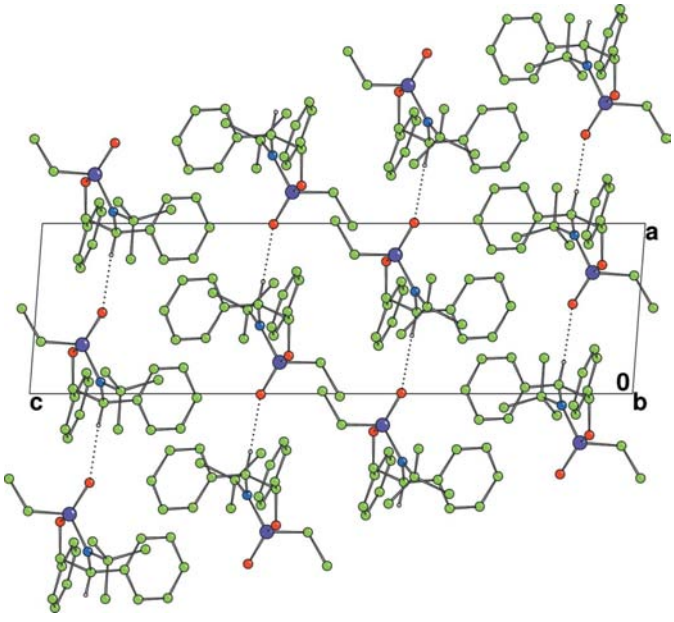

Figure 6
Part of the crystal structure of (II) showing one-dimensional chains running along the *a* axis.

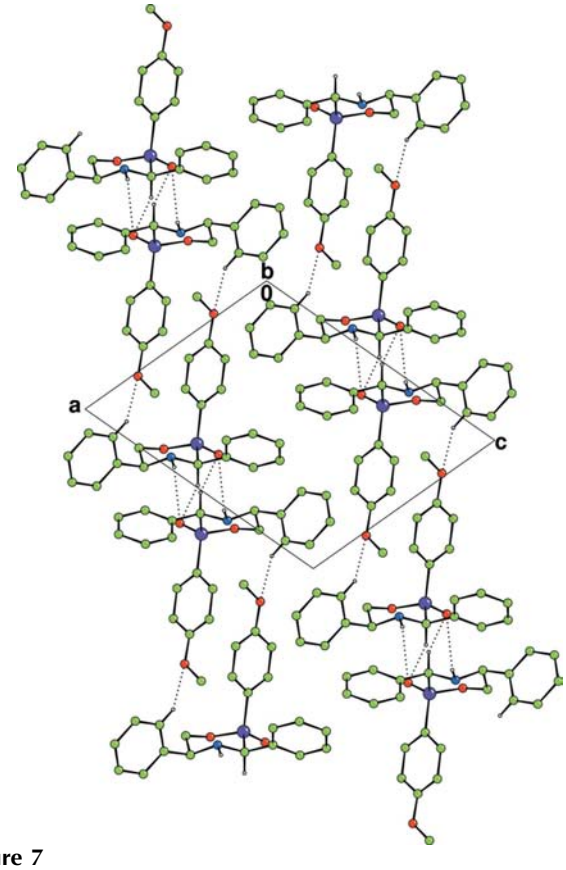

Figure 7
Part of the crystal structure of (VII) showing the stacking of hydrogen-bonded layers.

moieties on the P atom. The hydrogen-bonding geometry for the two independent enantiomorphs in the asymmetric unit is nearly equal: $D\cdots A$ = 3.196 (3) and 3.179 (3) Å, respectively; DH$\cdots A$ = 165 and 165°, respectively.

3.2.3. (2*R*,3*S*,5*S*)-3,5-Diphenyl-2-(4-methoxyphenyl)-1,4,2-oxazaphosphorinane 2-oxide (VII). The structure of (VII) forms two-dimensional networks of weakly hydrogen-bonded molecules. Fig. 7 shows the stacking of the layers that are perpendicular to the c^* axis. Fig. 8 shows a view perpendicular to the c^* axis and the formation of large $R_2^2(21)$ and $R_4^4(30)$ rings. Three different weak hydrogen-bond interactions can be distinguished. The phosphoryl O7 participates as an acceptor in the network by forming molecular chains along the *b* axis which are linked to parallel chains by weak bonding between the methoxy oxygen and a phenyl hydrogen. The phosphoryl oxygen is a bifurcated hydrogen-bond acceptor and with D—H$\cdots A$ angles and distances of 117.96 (7)° and 2.543 (3) Å for the N4—H31 donor moiety, and 118.00 (8)° and 2.568 (4) Å for the C3—H32 donor moiety, respectively, this interaction is weaker than the other phosphoryl hydrogen bonds found in this series. Between parallel layers there are no significant interactions.

3.2.4. (2*R*,3*S*,5*S*)-3,5-Diphenyl-1,4,2-oxazaphosphorinane 2-oxide (IX). The strongest hydrogen bonds in the present two series of cyclic oxazaphospholidines and oxazaphosphinanes are found in the structure of (IX) and involve, apart from the O7 acceptor, the N4 donor that is located on the opposite side of the oxazaphosphorinane ring. The attraction is so strong that the center of the H22 electron cloud is significantly shifted towards the O7 hydrogen acceptor, resulting in an N4—H22 distance of 1.052 Å, much longer than the accepted distance of 0.85 Å for Nsp^3—H distances. The D—H$\cdots A$ angle, 148.75 (10)°, is significantly shifted from that calculated for a geometrically placed H22 proton that is not involved in a weak bonding interaction, *i.e.* 95.70 (10)°. Fig. 9 shows that the *C*(5)

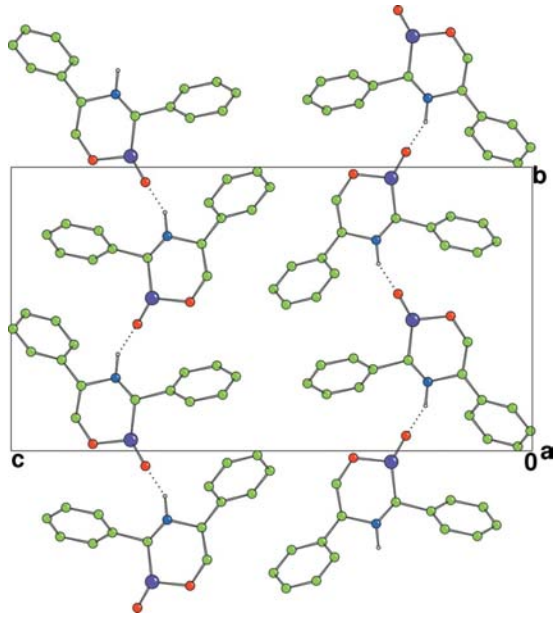

Figure 9
Part of the crystal structure of (IX) showing one-dimensional chains running along the *b* axis. CH$\cdots\pi$ interactions have not been indicated because this would give the false impression of their being intermolecular in nature. See Fig. 10.

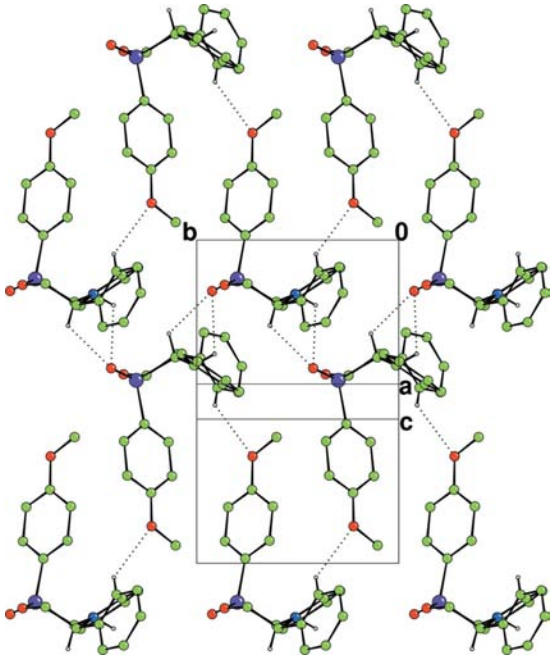

Figure 8
Part of the crystal structure of (VII) showing the two-dimensional network of hydrogen-bonded molecules perpendicular to the c^* axis.

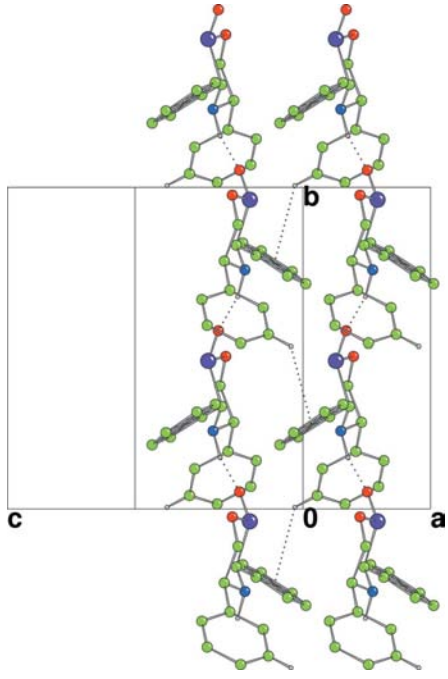

Figure 10
Part of the crystal structure of (IX) showing one-dimensional chains running along the *b* axis and additional linking of chains by CH$\cdots\pi$ interactions in the direction of *a*.

chains run along the *b* axis and are symmetry related by a twofold screw axis along that axis. There are no significant hydrogen-bond interactions between parallel chains in the *cb* plane. However, in a direction perpendicular to this plane, chains are linked by CH$\cdots\pi$ interactions between the centroid (or *Cg*) of one of the phenyl moieties and the H34 atom of the other moiety on a different chain, the H34—*Cg*3 distance being 2.960 (3) Å and the *D*—H$\cdots$*A* angle 131.81 (7)° (Fig. 10). In the classification of Malone *et al.* (1997) this is a type III interaction.

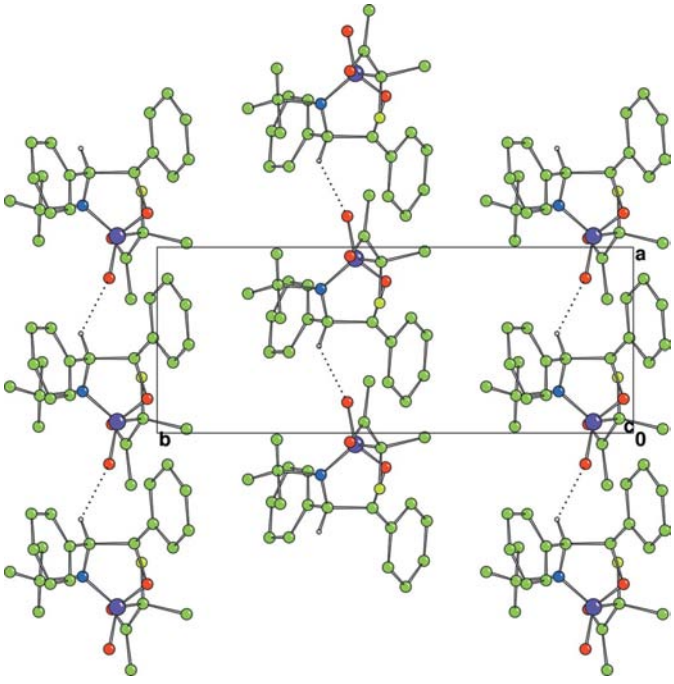

Figure 11
Part of the crystal structure of (III) showing one-dimensional chains running along the *a* axis.

3.2.5. (III)–(VI) and (VIII). Running *C*(5) chains along the *a* axis are also found in the structure of the *SSRS*/*RRSR* molecule (III), (±)-(2*S*,4*S*,5*R*)-3-*tert*-butyl-4,5-diphenyl-2-(1*S*)-1-fluoro-1-methyl-2-oxopropyl-1,3,2-oxazaphospholidine 2-oxide (Fig. 11), whereas in a diastereomer of molecule (III), *i.e.* molecule (IV), (±)-(2*S*,4*S*,5*R*)-3-*tert*-butyl-4,5-diphenyl-2-(1*R*)-1-fluoro-1-methyl-2-oxopropyl-1,3,2-oxazaphospholidine 2-oxide, linear *C*(5) chains run along the *b* axis, as is depicted in Fig. 12. In comparison to molecules (III) and (IV), molecule (V), (±)-(2*S*,4*S*,5*R*)-3-*tert*-butyl-4,5-diphenyl-2-(1*S*)-1-methyl-2-oxopropyl-1,3,2-oxazaphospholidine 2-oxide, differs with respect to the functional group linked to the P atom; the fluoro-methyl group has been replaced by an unsubstituted methyl group. The hydrogen-bonded network that is formed (see Fig. 13) contains two different rings, $R_4^4(28)$ and $R_4^4(30)$. The supramolecular structure of (VI), (±)-(2*R*,4*S*,5*R*)-2-benzyl-3-*tert*-butyl-4,5-diphenyl-1,3,2-oxazaphospholidine 2-oxide, is an exception, because no linear chains linked by weak phosphoryl CH$\cdots$O hydrogen bonds are formed. Instead a dimeric structure is created consisting of two symmetry-related molecules (VI) forming a hydrogen-bonded network containing a $R_2^2(6)$ ring and two symmetry-related $R_2^2(8)$ rings (Fig. 14). The structure of (VIII), (2*S*,3*S*,5*S*)-2,3,5-triphenyl-1,4,2-oxazaphosphorinane 2-oxide, forms one-dimensional chains along the *a* axis as do most of the five-membered oxazaphospholidine compounds (I)–(V).

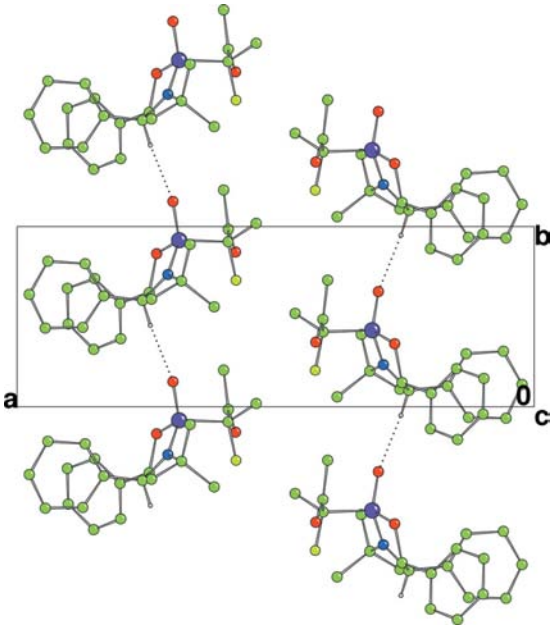

Figure 12
Part of the crystal structure of (IV) showing one-dimensional chains running along the *b* axis.

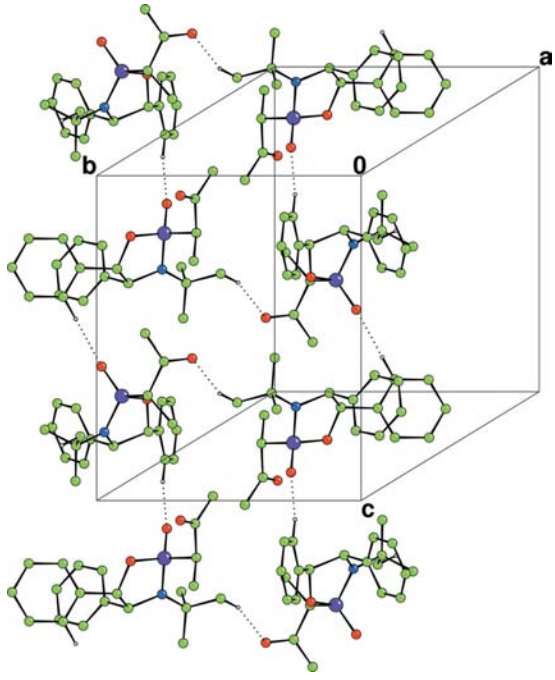

Figure 13
Part of the crystal structure of (V) showing one-dimensional chains running along the *b* axis and linking between adjacent chains *via* an oxopropyl oxygen to *tert*-butyl hydrogen interaction.

Fig. 15 shows that adjacent chains are symmetry-related by a twofold screw axis along *a*.

4. General discussion

The predominant features in the structures of the nine cyclic oxazaphospholidines and oxazaphosphinanes are the linear infinite chains formed by weak hydrogen bonds between the phosphoryl oxygen acceptor and carbon, or nitrogen donors on the opposite side of the molecule. In only one case, *i.e.* in the structure of molecule (VI), is a dimeric-type structure found without chains. There are two factors playing a role in how the supramolecular structure is built. First the P═O hydrogen-acceptor moiety has a tendency to form a hydrogen bond with the most acidic donor group available. Thus, in the oxazaphosphinanes the NH group becomes available as the donor group – while it is unavailable in the cyclic oxazaphospholidines, see (I)–(IX); in two of the three cases it is actually used to form hydrogen bonds. In the oxazaphospholidines only sp^2 and sp^3 C atoms act as potential donor groups, for which the energetic difference is only small and thus a second factor becomes important, *i.e.* the steric hindrance owing to the asymmetric environment of the P═O moiety. In the supramolecular structures of the diastereomer couples (I) and (II), and (III) and (IV), respectively, the donor groups for the phosphoryl oxygen acceptor are the same carbon C4 in each case, which is located on the other side of the ring. The asymmetric environments of the P2 and C4 centres are, however, different, giving the possibility of structure (II) developing strictly linear chains, since the P2═O and C4—H50 bonds are nearly antiparallel, whereas they are aligned in nearly parallel fashion for structure (I) yielding zigzag chains. Steric hindrance is also possibly the reason why in molecule (VIII) the NH group does not act as a donor moiety but rather the somewhat less acidic sp^3 C4 carbon. The three phenyl moieties in (VIII), see Fig. sup-viii of the supplementary data, are nearly perpendicular to the oxazophosphinane ring, as well as the P═O and the C4—H bonds, but the N—H bond is approximately parallel to the ring. Making a NH···P═O hydrogen bond would mean that the phenyl moieties of adjacent molecules are perpendicular to each other, whereas for a CH···P═O bond they are in parallel configuration. In the structure of (IX), with a relatively strong NH···P═O bond, this situation does not occur, because now the P═O moiety has a very open environment without the phenyl moiety.

The O═P hydrogen acceptor is to be considered as relatively weak; indeed, a limited search of the CSD by Forristal *et al.* (2001) has already shown a weak clustering of normalized H···O═P distances around 2.8 Å, which are considered to be consistent with a weak hydrogen-bonded interaction. A more complete CSD search looking for possible hydrogen interactions with a P═O hydrogen acceptor group and C, N or O bonded to P, shows only a very slight preference for the larger D—H···O angle as a function of the H···O distance. Represented in Fig. 16 is the normalized cubic distance function $R^3_{HO} = [d(H\cdots O)/(r_H + r_O)]^3$ with r_H and r_O the van der Waals radii for H and O, respectively ($r_H = 1.20$ Å and $r_O = 1.52$ Å; Bondi, 1964) *versus* the angle as $1 - \cos(D{-}H\cdots O)$, as explained by Lommerse *et al.* (1996). The hits from the search only involve non-disordered structures with the hydrogen positions renormalized to their neutron values. What is striking is that the spatially normalized hydrogen-bond distance R^3_{HO} spans a large interval

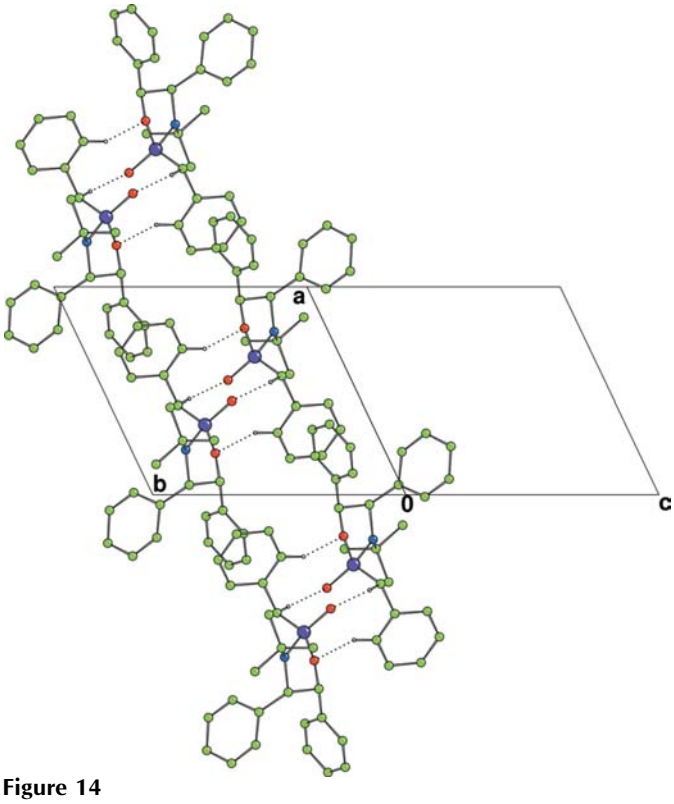

Figure 14
Part of the crystal structure of (VI) showing a dimeric structure formed by four weak hydrogen-bond interactions.

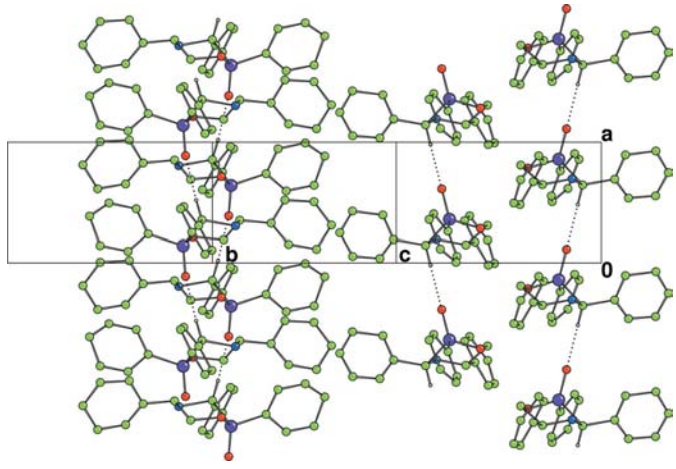

Figure 15
Part of the crystal structure of (VIII) showing one-dimensional chains running along the *a* axis.

between 0.20 and 1.30, without showing a very marked trend *versus* the angle.

A more limited search of the CSD (Version 5.28, Allen, 2002) gives 46 and 16 compounds with oxazaphospholidine and oxazaphosphinane rings, respectively. Among the structures containing oxazaphospholidine rings there are only three in which no CH···O═P or NH···O═P interactions can be identified; for the oxazaphosphinane ring containing structures this number equals 2. The mean H···O distance, regardless of whether the donor is C or N, is 2.542 Å from 93 observations, which is in agreement with that found for structures (I)–(VI). The lowest distance is 2.282 Å for refcode SIMTUD (Seidel *et al.*, 1990), which is approximately as short as the shortest distances in Table 2, taking into account the variability for which the proton positions are determined. The oxazaphosphinane series has only nine observations with a mean H···O distance of 2.248 Å, with some low NH···O═P distances of 1.789 and 2.021 Å for refcodes HIQLIC (Saint-Clair *et al.*, 1999) and FEWHOE (Makaranets *et al.*, 1987), respectively. The tendency towards lower H···O═P is equally well observed in the three oxazaphosphinane structures of this paper. The tendancy towards the formation of infinite one-dimensional hydrogen-bonded polymers is less pronounced in the CSD series than in the structures described in this paper, probably because of a wider variety of functional groups attached to the rings.

Although a statistical analysis of P═O···H contacts is not very conclusive with respect to the question whether hydrogen bonds are really formed, a close analysis of the supramolecular bond patterns in the individual structures reveals that there is not much doubt that this is indeed the case. The most interesting phenomenon observed is that, at least for cyclic oxazaphospholidines and oxazaphosphinanes, the formation of P═O···H hydrogen bonds results in molecular chains that can be linear or zigzag, but which propagate in one direction. Henn *et al.* (2004) have reported DFT calculations on CH···O═P interactions between $CHCl_3$ and a triphosphonic ester 1,3,5-$[P(O)(^iPrO)_2]_3C_6H_3$ and concluded that the hydrogen bonding is 'moderately' strong, 20.5 kJ mol^{-1}, comparable with the hydrogen-bond interaction of the water dimer (22.6 kJ mol^{-1}). The corresponding calculated charge transfer from the P═O group to the antibonding CH orbital is significant (0.014 a.u.), but substantially smaller than that in the water dimer (0.024 a.u.). At the same time, the CH···O angle appears to be as flexible owing to the high electrostatic character of the CH···O═P interaction, which is effectively in agreement with the absence of any trend in the scattergram of Fig. 16. Felemez *et al.* (2000) concluded from ^{31}P and ^{1}H NMR titration experiments on inositol phosphates and molecular modeling that the CH···O═P bond is relatively 'weak'.

With regard to the potential of phosphoryl-containing molecules in crystal engineering, it can be stated that this is relatively small because of its relative strength (weak to moderately strong) and of the flexibility of the CH···O angle. In this respect Henn *et al.* (2004) expect that CH···O═P (or NH···O═P) interactions play at least a role in the formation of the 'secondary' structure of phosphate-containing biomolecules. Structure prediction therefore remains difficult; even with prior knowledge of other similar structures one could hardly predict the resulting hydrogen-bonded structure. It is in this respect astonishing that in eight of the nine investigated structures *linear* molecular chains are formed and not more dimeric structures if the P═O bond is in an antiparallel orientation with respect to the *X*—H donor bond.

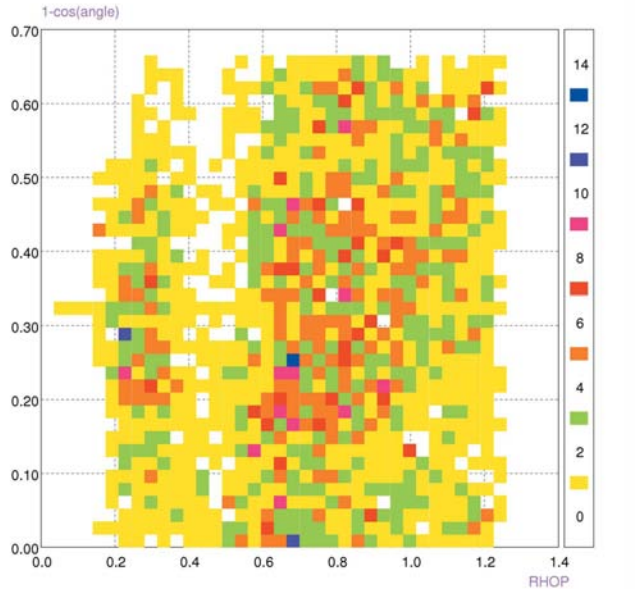

Figure 16
Scattergram of the spatially normalized hydrogen-bond distances (R^3_{HO}) *versus* the hydrogen-bond angle [represented as $1-\cos(D-H\cdots O)$] prepared by the statistical package *VISTA* (Version 2.1c, CSD; Allen, 2002).

Dr G. Vaughan of the European Synchrotron Radiation Facility (beamline ID11) is kindly thanked for assistance during the data collection of the two crystals (I) and (II). The data of crystals (III)–(IX) have been measured on several diffractometers of the Joint X-ray Scattering Service of the Institut Européen des Membranes and the Institut Charles Gerhardt of the Université de Montpellier II. Dr R. Astier is kindly thanked for collecting the datasets of some of the crystals.

References

Allen, F. H. (2002). *Acta Cryst.* B**58**, 380–388.
Altomare, A., Cascarano, G., Giacovazzo, C., Guagliardi, A., Burla, M. C., Polidori, G. & Camalli, M. (1994). *J. Appl. Cryst.* **27**, 435.
Bernstein, J., Davis, R. E., Shimoni, L. & Chang, N.-L. (1995). *Angew. Chem. Int. Ed. Engl.* **34**, 1555–1573.
Betteridge, P. W., Carruthers, J. R., Cooper, R. I., Prout, K. & Watkin, D. J. (2003). *J. Appl. Cryst.* **36**, 1487.
Bondi, A. (1964). *J. Phys. Chem.* **68**, 441–451.
Burla, M. C., Camalli, M., Carrozzini, B., Cascarano, G. L., Giacovazzo, C., Polidori, G. & Spagna, R. (2003). *J. Appl. Cryst.* **36**, 1103.
Cristau, H. J., Monbrun, J., Tillard, M. & Pirat, J. L. (2003). *Tetrahedron Lett.* **44**, 3183–3186.

Felemez, M., Bernard, P., Schlewer, G. & Spiess, B. (2000). *J. Am. Chem. Soc.* **122**, 3156–3165.
Flack, H. D. (1983). *Acta Cryst.* A**39**, 876–881.
Forristal, I., Lowman, J., Afarinkia, K. & Steed, J. W. (2001). *CrystEngComm*, **14**, 1–4.
Grembecka, J., Mucha, A., Cierpicki, T. & Kafarski, P. (2003). *J. Med. Chem.* **46**, 2641–2655.
Henn, M., Jurkschat, K., Mansfeld, D., Mehring, M. & Schürmann, M. (2004). *J. Mol. Struct.* **697**, 213–220.
Kolodiazhnyi, O. I. (1998). *Tetrahedron Asym.* **9**, 1279–1332.
Larson, A. C. (1970). *Crystallographic Computing*, edited by F. R. Ahmed, pp. 291–294. Copenhagen: Munksgaard.
Lommerse, J. P. M., Stone, A. J., Taylor, R. & Allen, F. H. (1996). *J. Am. Chem. Soc.* **118**, 3108–3116.
Macrae, C. F., Edgington, P. R., McCabe, P., Pidcock, E., Shields, G. P., Taylor, R., Towler, M. & van de Streek, J. (2006). *J. Appl. Cryst.* **39**, 453–457.
Makaranets, B. I., Polynova, T. N., Porai-Koshits, M. A. & Il'ichev, S. A. (1987). *J. Struct. Chem.* **27**, 603–609.
Malone, J. F., Murray, C. M., Charlton, M. H., Docherty, R. & Lavery, A. J. (1997). *J. Chem. Soc. Faraday Trans.* **93**, 3429–3436.
Oxford Diffraction (2006). *CrysAlis CCD/RED*, Version 1.171.31.7. Oxford Diffraction Ltd, Abingdon, England.
Pirat, J.-L., Marat, X., Clarion, L., van der Lee, A., Vors, J.-P. & Cristau, H.-J. (2005). *J. Organomet. Chem.* **690**, 2626–2637.
Pirat, J.-L., Monbrun, J., Virieux, D., Volle, J.-N., Tillard, M. & Cristau, H. J. (2005). *J. Org. Chem.* **70**, 7035–7041.
Prince, E. (1982). *Mathematical Techniques in Crystallography and Materials Science.* New York: Springer-Verlag.
Saint-Clair, J.-F., Siméon, F., Villemin, D. & Averbuch-Pouchot, M.-T. (1999). *Acta Cryst.* C**55**, 588–590.
Seidel, H. M., Freeman, S., Schwalbe, C. H. & Knowles, J. R. (1990). *J. Am. Chem. Soc.* **112**, 8149–8155.
Siemens (1993). *SMART*. Siemens X-ray Instruments, Inc., Madison, Wisconsin, USA.
Siemens (1995). *SAINT*. Siemens X-ray Instruments, Inc., Madison, Wisconsin, USA.
Smaalen, S. van, Palatinus, L. & Schneider, M. (2003). *Acta Cryst.* A**59**, 459–469.
Spek, A. L. (2003). *J. Appl. Cryst.* **36**, 7–13.
Volle, J.-N., Virieux, D., Starck, M., Monbrun, J., Clarion, L. & Pirat, J.-L. (2006). *Tetrahedron Asym.* **17**, 1402–1408.
Watkin, D. (1994). *Acta Cryst.* A**50**, 411–437.
Watkin, D. J., Prout, C. K. & Pearce, L. J. (1996). *CAMERON*. Chemical Crystallography Laboratory, Oxford, UK.